# Experimental cell for molecular beam deposition and magnetic resonance studies of matrix isolated radicals at temperatures below 1 K

S. Sheludiakov, J. Ahokas, O. Vainio, J. Järvinen, D. Zvezdov, S. Vasiliev, V. V. Khmelenko, S. Mao, and D. M. Lee

# Experimental cell for molecular beam deposition and magnetic resonance studies of matrix isolated radicals at temperatures below 1 K

S. Sheludiakov,[1,a)] J. Ahokas,[1] O. Vainio,[1] J. Järvinen,[1] D. Zvezdov,[1,b)] S. Vasiliev,[1] V. V. Khmelenko,[2] S. Mao,[2] and D. M. Lee[2]

[1]*Wihuri Physical Laboratory, Department of Physics and Astronomy, University of Turku, 20014 Turku, Finland*
[2]*Department of Physics and Astronomy and Institute for Quantum Science and Engineering, Texas A&M University, College Station, Texas 77843, USA*

We present the design and performance of an experimental cell constructed for matrix isolation studies of H and D atoms in solid $H_2/D_2$ films, which are created by molecular beam deposition at temperatures below 1 K. The sample cell allows sensitive weighing of the films by a quartz microbalance (QM) and their studies by magnetic resonance techniques in a strong magnetic field of 4.6 T. We are able to regulate the deposition rate in the range from 0.01 to 10 molecular layers/s, and measure the thickness with $\approx 0.2$ monolayer resolution. The upper QM electrode serves as a mirror for a 128 GHz Fabry-Perot resonator connected to an electron spin resonance (ESR) spectrometer. H and D atoms were created by RF discharge *in situ* in the sample cell, and characterized by ESR and electron-nuclear double resonance. From the magnetic resonance measurements we conclude that the films are smooth and provide homogeneous trapping conditions for embedded atoms. The current sample cell design also makes it possible to calibrate the ESR signal and estimate the average and local concentrations of H and D radicals in the film. © *2014 AIP Publishing LLC*. [http://dx.doi.org/10.1063/1.4875985]

## I. INTRODUCTION

Thin molecular hydrogen films are attracting significant interest in low-temperature physics and chemistry. Having small mass and weak intermolecular potentials the solid hydrogens (especially solid para-$H_2$) are good host matrices for high resolution spectroscopic studies of free radicals.[1] Smooth surfaces of solid $H_2$ may serve as good substrates for studies of high density 2D electron gases.[2] It turns out that the preparation of a smooth and thin ($\lesssim 10\ \mu m$) films of solid molecular hydrogen is a challenging task because of its non-wetting behavior on metal surfaces below the triple point.[3] This limits the thickness of the film grown in equilibrium with the vapor to a few molecular layers, above which clusters of bulk polycrystallines are formed. Another approach is to use quench-condensing method, where an intense flux of molecules is flushed onto a substrate with a temperature about 1.5 K.[4] This method allows formation of rather homogeneous films, but with thicknesses of the order of a fraction of mm. Since the deposition rate is relatively high, this leads to a strong overheating of the matrix, and limits the deposition temperature above 2–3 K. The thickness of the films is hard to control and measure during fast deposition. A quartz microbalance (QM) is widely used for measuring the film thickness deposited at room temperature. This technique has been effectively used in studies of 2D superfluidity[5] and surface wetting[6] at temperatures below 1 K. Quartz microbalances were also used for matrix isolation studies[7,8] combined with

X-band electron spin resonance (ESR), but at substantially higher temperatures of a few K.

In this paper we describe construction and performance of the sample cell (SC) designed for studies of H and D atoms in solid $H_2$ and $D_2$ by methods of high field electron and nuclear magnetic resonance at temperatures down to 70 mK. We utilize a new type of molecular beam method based on the sublimation of solid molecular hydrogen at source temperatures of 4–6 K. Regulating the temperature of the sources, we can control the deposition rate with high resolution at very small rates. This allows the substrate temperature to be kept substantially below 1 K and provides conditions for preparation of smooth and homogeneous hydrogen films. The quartz microbalance crystal serves as a substrate for the films, and at the same time as a flat mirror of 128 GHz Fabry-Perot resonator (FPR). The open geometry of the resonator allows arranging the RF coils with fringing field penetrating the deposited films. All these features provide an opportunity of simultaneous measurement of the film mass, and magnetic resonance characterization of the atoms which we create inside the films by the RF discharge.

The use of electron dissociation technique gives an opportunity to create samples with high concentrations of H radicals for studying macroscopic quantum phenomena and exchange tunneling chemical reactions at ultralow temperatures.[9–11] The QM mass measurement along with the possibility of calorimetric calibration of the ESR signal allows quantifying relative concentrations of atomic radicals in the film. Extracting local concentrations from the ESR linewidth and dipolar shift from the ESR gas lines[11] makes it possible to probe atomic radical distributions in the film and search for evidence of possible hydrogen atom clustering in the sample.

---

a)Electronic mail: seshel@utu.fi.
b)Also at Kazan Federal University, 420008, 18 Kremlyovskaya St, Kazan, Russia.

## II. SAMPLE CELL

The experiments are carried out in the sample cell shown in Fig. 1. Its construction is based on thoroughly revised designs of the SCs used in our previous experiments on atomic radicals of H in solid molecular hydrogen films.[10–12] The experimental cell consists of a main sample cell volume with a Fabry-Perot resonator and two sublimation-type sources for the beams of $H_2$ and $D_2$ molecules. The SC is thermally anchored to the mixing chamber of an Oxford 2000 series dilution refrigerator and located in the center of a 4.6 T superconducting magnet with homogeneity of $2 \times 10^{-6}$ in 1 cm$^3$ and a large (100 mm) bore.

The main diagnostic tools in our experiments are the ESR operating at 128 GHz, nuclear magnetic resonance (NMR), and mass measurement by the quartz crystal microbalance. Hydrogen films are deposited onto the QM which also works as a flat mirror of the semi-confocal FPR of the ESR spectrometer, making it possible to carry out studies by both methods simultaneously.

The sample cell was designed to be modular, to ease testing, assembly, and future modifications of the rather complex vacuum system. The main sample cell volume consists of 2 vacuum tight volumes separated by the QM (cell volume and helium volume). Two sublimation chambers are connected to the cell volume for making the $H_2$ ($D_2$) coating. In each sublimation chamber the RF coils were installed which allow controlling loading of the source with molecular gases. The sample cell is made of high purity copper and has altogether 7 indium seals excluding capillary connections. Several coaxial feedthroughs were build for running DC and RF-measurements.

### A. Fabry-Perot resonator

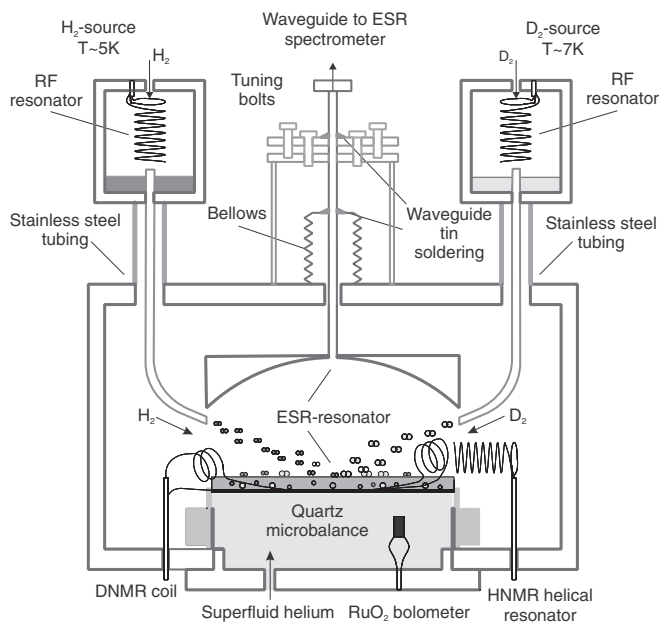We have chosen an open Fabry-Perot type of the mm-wave resonator, because it provides the possibility of
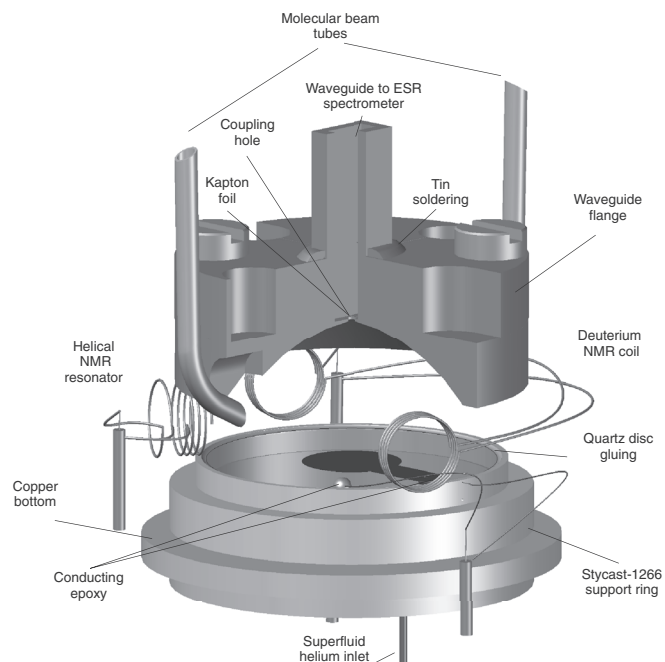


FIG. 2. Fabry-Perot resonator with installed NMR coils. The top electrode of the QM is shown transparent.

combining several other diagnostic tools with the ESR. Having nearly the same Q-factor as cylindrical cavities, the FPR allows introducing molecular beam lines and generating RF fields for NMR of H and D atoms in the sample located at the maximum of mm-wave field. In addition, the lower flat FPR mirror also serves as an electrode of the quartz microbalance with the mass-sensitive area coinciding with the mm-wave field maximum (Fig. 2), as described in Sec. II B. The second, upper FPR mirror is semi-spherical. It is manufactured out of high purity copper and has a 9 mm radius of curvature, 12 mm aperture, and 0.5 mm diameter/0.15 mm thick iris in the center for coupling it to the waveguide. The mirror is bolted to a waveguide flange. The SC volume is sealed by a thin Kapton foil glued to the waveguide flange with Stycast 1266. The upper mirror can be moved ±1 mm by pulling the waveguide up or down with a special tuning mechanism located outside the sample cell (Fig. 1). This allows a smooth tuning of the resonator frequency by 4–5 GHz at room temperature. An $\approx$0.5 m long oversized waveguide connects the FPR to the mm-wave bridge of the ESR spectrometer, which is thermally anchored to the 1 K pot of the dilution refrigerator. The waveguide is composed of several copper and thin-walled CuNi sections for thermal insulation. The sections are thermalized to the 0.1 K and 0.7 K stages of the refrigerator. Overall loss between the SC and mm-wave bridge is less than 5 dB. Beams of molecular $H_2$ and $D_2$ enter into the FPR volume via two slots in the upper mirror (Fig. 2). The beam lines are directed at the center of the flat FPR mirror (i.e., quartz microbalance) where the mm-wave field and QM-mass sensitivity have maxima. The resonator is tuned at room temperature to the $TEM_{005}$ mode. Cooling to 4.2 K shifts the resonator frequency by $\approx$2 GHz up, and since the spectrometer operating band is $128.3 \pm 0.4$ GHz, this shift should be taken into
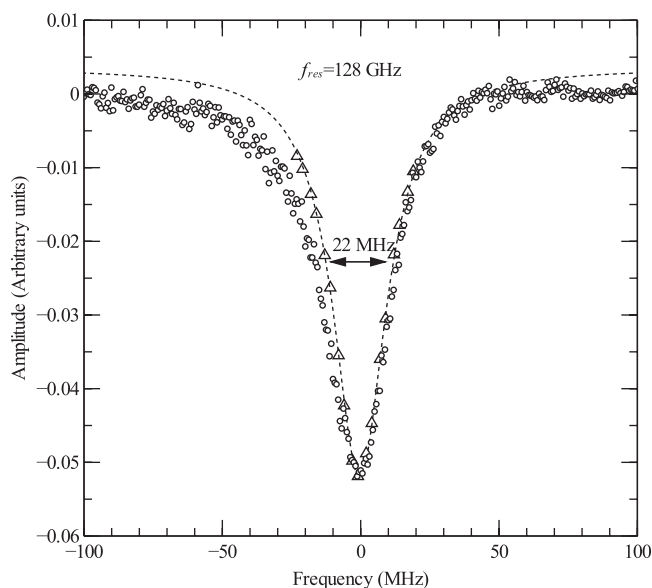


FIG. 1. Sample cell schematic.

FIG. 3. Resonance curve of FPR at 300 K (circles) and 300 mK (triangles) extrapolated by a Lorentz function (dashed line).

account while tuning the resonator at room temperature.[13] The FPR resonator reflection curves recorded at room temperature and 300 mK are shown in Fig. 3. The data at 300 mK are obtained from the change of the ESR signal intensity while varying the mm-wave frequency. The Q-factor increases from 4700 at room temperature to 5800 at 300 mK.

## B. Quartz microbalance

To make the best choice for the QM, we tested products of several manufacturers. Usually, the electrodes of the commercial QMs are manufactured with Cr or Ni underlayers for better adhesion for the gold or silver electrodes.[14] Since we cannot use the materials with strong magnetization, we had to make electrodes ourselves from weakly magnetic metals. The other requirements for the quartz crystal were the highest possible Q-factor and clean and smooth surfaces of the crystals. These properties were found to be the best for quartz disks manufactured by LIT-phonon,[15] which are 11 mm diameter, 0.5 mm thick AT-cut quartz crystals operating in the shear mode at the fundamental frequency of ≈10 MHz. Both surfaces of the disk are polished to a sub-$\mu$m level providing a smooth substrate for hydrogen films. The QM electrodes (Fig. 2) were produced by sputtering a 15 nm thick copper layer for better adhesion of the main, 500 nm thick gold layer. The top electrode occupies nearly whole surface of the side ($d = 10.8$ mm). The oscillating area of the quartz sensitive to mass deposited on its surface is defined by the size of the bottom electrode. It has a key-hole shape with mass sensitive area of 4 mm in diameter. Since the skin-depth for 128 GHz is ≲100 nm the electrode thickness was made large enough to be non-transparent for mm-waves, and so as not to influence the FPR Q-factor. On the other hand, the thickness of the gold layer (500 nm) is substantially smaller than the skin depth for frequencies below 1 GHz, allowing efficient penetration of the RF field into the sample in the double resonance

experiments. Thick electrodes may also shift substantially the QM frequency and decrease its quality factor. In our case the effect of the electrodes was to shift the fundamental mode frequency by ≈0.5 MHz, and decrease the Q-value from 40 000 to 20 000. Electrical contacts of 50 $\mu$m diameter copper wires to the QM electrodes were made with Eccobond VSM silver epoxy near the disc edges. Heavy electrodes may introduce non-linearity to the QM response towards the mass load. We verified that our QM response was linear up to hydrogen film thicknesses of ≈10 $\mu$m by measuring its frequency during deposition at constant mass flux and temperature.

The next problem to solve was heat removal from the QM during the film deposition. Since we were aiming for film deposition onto a surfaces at temperatures below 1 K, and the surfaces of the QM should not be loaded by large mass, or clamped, this turned out to be a difficult task. We found a solution by arranging a separate chamber under the QM (helium volume), which could be filled with superfluid helium to flush the lower quartz surface. Superfluid behavior of helium and its films ensures a small loading effect on the QM, but provides very good convection of heat. To make vacuum tight connections of the QM separating two different chambers, we glued the quartz disk at its perimeter by Stycast 1266 epoxy to a support ring (Fig. 2). The ring, glued to the copper bottom of the SC, is machined from the same epoxy and its wall thickness is decreased to 0.2 mm at the top to reduce stress to the quartz resulting from different thermal expansion of the materials. To avoid breaking the quartz, one has to monitor the pressure difference above and below the quartz disc, which should not exceed 100 mbar. This requirement also limits the use of helium for heat removal to temperatures about 2.5 K because its vapor pressure increases significantly at higher temperatures. Typically about 4 mmol of He gas is condensed into the helium volume, which is enough to form a saturated film there. The presence of a helium film in the helium volume of the SC was monitored with a bolometer (Fig. 1), which was made from a $RuO_2$-chip suspended on thin superconducting wires, thus having a weak thermal link to the SC wall.

The QM frequency was monitored with room temperature electronics, utilizing a reflection type circuit and a standard FM technique similar to that of Lea et al.[16] The frequency of the excitation source is locked to the maximum of the QM-resonance curve with a feed-back controlled by computer. A modulation frequency of 90 Hz ($f <$ FWHM of the QM) was applied to prevent any influence on the Q-factor of the QM. The QM performance was tested both at the fundamental mode ($f = 9.7$ MHz) and at its overtones. We found out that the QM performed best at its 3rd harmonic ($f = 29.68$ MHz) where the $Q \approx 10^5$ and the mass sensitivity is nearly tripled. We also did not notice any decrease of the Q-factor after deposition of a hydrogen film of sub-$\mu$m thickness on the QM. Long term frequency stability of the QM was measured at 100 mK with a 300 nm $H_2$ film and with the absence of helium in both volumes. Stability of less than 1 Hz was achieved during 15 h of measurements (Fig. 4). The total frequency change due to cooling of the cell from 1 K to 100 mK was about 20 Hz. Deposition of 1 molecular layer of $H_2$ shifts the QM frequency by ≈0.7 Hz down for the fundamental mode. Working at the 3rd harmonic and having
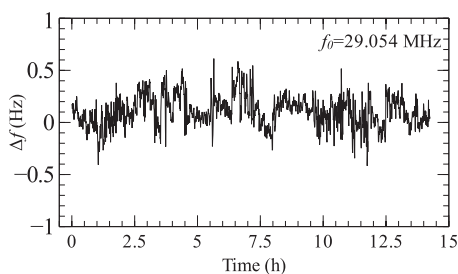
FIG. 4.  Long-term QM-frequency stability at 100 mK.

short-term frequency stability of 0.4 Hz we are able to measure the film thickness with about a 0.2 monolayer resolution.

## C. NMR resonators

Two NMR resonators are installed close to the FPR to carry out electron-nuclear double resonance (ENDOR) studies of the samples (Figs. 1 and 2). One of them (HNMR) is designed for the excitation of NMR transition of H atoms, which occur at $f \approx 910$ MHz in a 4.6 T field. The second resonator (DNMR) matches the NMR transition of atomic deuterium at $\approx 139$ MHz. The HNMR is a helical $\lambda/4$ resonator grounded at one end and inductively coupled to the coax line. Such resonators are usually used at frequencies $\sim 1$ GHz where it is difficult to build LC-circuits from discrete elements. Typically the resonance frequency shifts up by $\approx 8$ MHz due to cooling down to cryogenic temperatures. This shift is taken into account when tuning the resonator at room temperature. The HNMR has a Q-factor of $\approx 60$. The NMR of deuterium requires a substantially lower frequency. Therefore the DNMR is based on an LC circuit with a varactor-based tuning mechanism similar to that used in Ref. 17. Two coils connected in series and located symmetrically relative to the FPR axis form the DNMR inductor (Figs. 1 and 2). This Helmholtz-type coil configuration helps to improve the RF-field homogeneity at the center of the flat mirror of the FPR (Fig. 1). Even though the samples are located outside the NMR resonators, the fringing RF-field is strong enough to perform ENDOR at RF powers of 1–100 $\mu$W, which do not exceed the cooling power of dilution refrigerator below 0.5 K.

The coil of the HNMR can be also used to run the RF-discharge in the helium vapors needed to produce H radicals in $H_2$ films. This method was initially developed for producing atomic hydrogen gas,[18] but can also be used for dissociation of hydrogen molecules inside the $H_2$ matrix.[11] RF pulses ionize helium atoms and produce electrons with a characteristic kinetic energy of about 100 eV. This energy appears to be enough for electrons to penetrate through the helium film and dissociate hydrogen molecules into atoms at the effective depth of the $H_2$ film up to 100 nm. The method is very efficient and allows us to produce samples with maximum H densities in $H_2$ films of $2 \times 10^{19}$ cm$^{-3}$.[11,12] RF-power is supplied to the resonator in short pulses with a duration of 0.01–0.3 ms and a 20–30 Hz repetition rate. Since molecular hydrogen has a very small vapor pressure below 1 K, a small quantity ($\gtrsim 20$ $\mu$mol) of He gas has to be introduced into the cell volume to start the discharge. Switching on the discharge can

be seen with the oscilloscope by observing the change of the signal reflected from the RF-resonator. A broad cyclotron resonance line of free electrons appears in the ESR spectrum at the same time.

## D. Molecular sources

Incomplete wetting of metallic surfaces by hydrogen below the triple point makes $H_2$-film deposition onto metallic substrates very challenging. Quench-condensing of $H_2$ gas onto cold substrate traditionally used in matrix isolation usually results in having films with a thickness of fractions of mm.[1] A high deposition rate complicates controlling of the film thickness and keeping the substrate cold enough to prevent $H_2$ film coagulation. An alternative method was discovered in our previous experiments.[10–12] In these experiments solid molecular hydrogen films were prepared by recombination of the gas-phase atoms on a Mylar substrate. This allowed growing ultra-pure, smooth, and homogeneous hydrogen films, but with an extremely slow rate of about 1 monolayer/h. Since the low deposition rate and substrate temperature turned out to be key features, we suggested use of a new type of molecular source based on the sublimation of $H_2$ or $D_2$ molecules at temperatures 4–6 K. Easily adjusted deposition rates (0.01–10 monolayers/s) allow growth of smooth and homogeneous molecular hydrogen and deuterium films of various thickness in reasonable times. Using molecules sublimated from solid hydrogen rather than hot $H_2$ and $D_2$ gases makes it possible to significantly decrease the amount of heat delivered to the substrate during deposition.

The $H_2$ and $D_2$ sublimation chambers, later referred as the $H_2$ and $D_2$ sources, are placed about 7 cm above the level of the QM and connected to the top flange by a thermally insulating support. The support is made by connecting three stainless steel tubes $d = 2, 3$, and 5 mm with wall thickness of 0.1 mm in series, concentrically one inside another, in order to provide good thermal insulation while keeping the distance from the sources to the SC top rather short. Molecular vapors are directed to the QM via thin copper capillaries $d = 1.2/0.5$ mm going into the SC along the axis of the stainless steel support. The sublimation chambers can be heated to temperatures above 5 and 7 K where the vapor pressures of $H_2$ and $D_2$ become large enough to provide substantial flux of molecules into the SC. The sample cell temperature can be kept $\lesssim 0.7$ K during the molecule deposition procedure. Molecular hydrogen isotope samples are loaded into the sources from room temperature through capillaries electrically heated to temperatures above the corresponding melting points. Because the sources must be kept below 4 K during loading, weak thermal links were made to the heat exchanger with the diluted $^3$He-$^4$He stream before it enters the still of the dilution refrigerator. This method of heating the sources does not disturb the fridge operation and only increases the circulation rate. Unfortunately, the rather high minimum temperature, 0.5 K, of the sources limits the lowest temperature of the SC to about 70 mK despite the thermal insulation. Helical resonators ($f \approx 350$ MHz, Fig. 1) installed in both sources can be used to monitor loading of the gases due to the change of the dielectric constant shifting the resonator frequencies down. A

1 MHz shift roughly corresponds to 2 mmol of the gas condensed in the source.

Running the RF discharge in the sample cell does not only dissociate molecules in the solid films. Some of the dissociated atoms leave the solid matrix and enter the SC space. Thus a small flux of atoms is generated into the SC volume above the solid hydrogen film. This type of cold atomic hydrogen gas source is well known and has been used in several laboratories.[18] The SC HNMR coil and helical resonators in the sublimation chambers can be used for this purpose. The ESR signal from atoms of the gas phase at low density provides a good reference for accurate measurement of the *g*-factor and hyperfine constant, the main parameters obtained in the magnetic resonance of the matrix isolated atoms.

The setup presented here provides the possibility of measuring the absolute number of atoms and molecules in the samples by independent methods. The atomic density can be inferred from the ESR absorption integrals while the number of molecules can be extracted from the QM signal. Absolute calibration of the ESR absorption integrals can be done calorimetrically by measuring the recombination of H atoms in the gas phase.[19] Every recombination event between two hydrogen atoms is accompanied by releasing 4.5 eV of energy so that the gas ESR-line area decrease can be associated with the amount of heat released.

## III. PERFORMANCE TESTS

A typical procedure for $H_2$-deposition on the surface of the QM is shown in Fig. 5. The cell temperature is stabilized at about 0.5–0.7 K, depending on the molecular source temperature. By varying temperature of the $H_2$ molecular source between 4 and 6 K we were able to change the deposition rate by 3 orders of magnitude (Fig. 6). The corresponding $H_2$ molecular flux onto QM varied between $8 \times 10^{12}$ and $4 \times 10^{15}$ molecules/s.

We tried to determine the importance of cooling the lower QM surface by superfluid helium. We found that in the absence of helium in the helium volume, at rates higher than about 4 monolayers/s some of the $H_2$ molecules bounced back from the QM and stuck to the spherical mirror of the FPR.
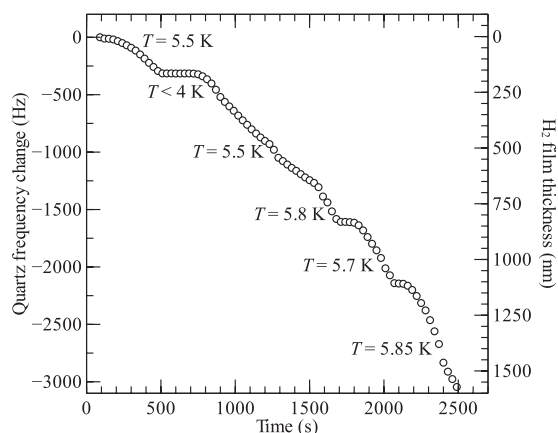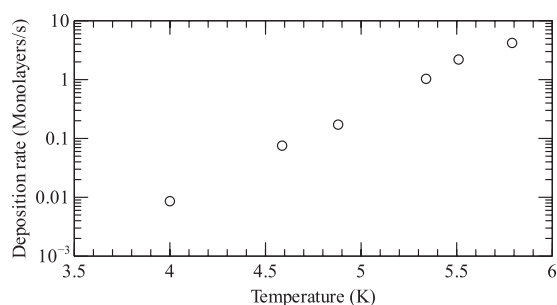


FIG. 6. Dependence of the deposition rate of $H_2$ film on the $H_2$-source temperature.

This indicated that the surface got substantially overheated at high deposition rates. The presence of a molecular layer on the spherical mirror was found by applying the magnetic field gradient. The ESR lines were split into two peaks, corresponding to the films on each mirror.[11]

A layered sample of H-$H_2$ was prepared to study the film structure. First a 10 nm $H_2$-film was deposited and atomic radicals were created in the film by running the RF-discharge. Then a $H_2$ film of double thickness was added and the discharge in the SC was started again. This procedure was repeated several times. The ESR signal of H atoms as a function of $H_2$ film thickness is shown in Fig. 7. The ESR absorption signal grows monotonically with the film thickness up to about 100 nm and saturates at larger thicknesses. On the basis of this observation we can conclude that electrons from the discharge effectively penetrate into the $H_2$ film up to about 100 nm. Monotonic dependence of the ESR signal on the film thickness provides evidence for a layered structure of the resulting film and proves that no clusterization occurs.

A typical ESR spectrum of atomic hydrogen and deuterium stabilized in solid $H_2/D_2$ matrices is shown in Fig. 8. Hyperfine interaction between nuclear and electron spins leads to a doublet of lines for atomic hydrogen and a triplet for atomic deuterium. Hydrogen lines are separated by 507 G in the field of 4.6 T, while atomic deuterium lines only by ~78 G.

In order to study film homogeneity, we analyzed the cage effect on the atomic H and D impurities. Electrons of the host molecules interact with the electrons of the impurity atoms via attractive van der Waals interactions and Pauli repulsion.[20] The former or latter prevails depending on the trapping site
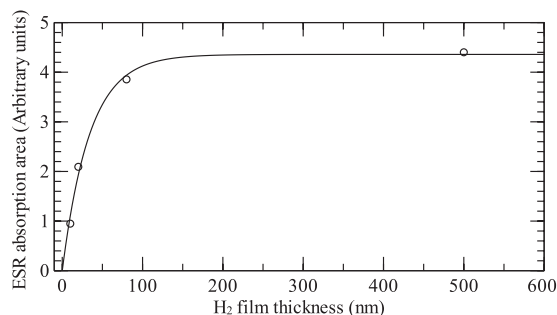


FIG. 5. Dependence of QM frequency and thickness of $H_2$ film on time during process of $H_2$ film deposition at different temperatures.



FIG. 7. Dependence of ESR signal area of H atoms (open circles) on the $H_2$ film thickness.
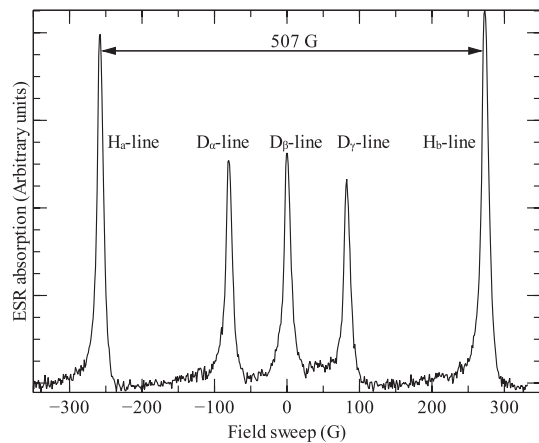
FIG. 8. ESR spectra of H and D atoms stabilized in the $H_2$-$D_2$ matrix at T = 300 mK.

occupied by the impurity. It distorts electron clouds of the impurities affecting the hyperfine constant $A$. NMR is very sensitive to the change of $A$ and is usually used to probe it, and the NMR transition width may provide information regarding how disordered the film is. Very narrow NMR transitions, $\Delta f = 20$ KHz, observed in our experiments give evidences for very high film homogeneity and uniform trapping conditions provided to the impurity atoms (Fig. 9). Larger shift for the H in $D_2$ from the free atom resonance indicates stronger coupling to the lattice.[11,20]

The relative concentrations of H atoms in $H_2$ matrices can be calculated from the absolute measurement of the quantity of H atoms by ESR and the detection of the quantity of $H_2$ molecules by the QM. Alternatively, local concentrations of H atoms can be determined from the analysis of the ESR linewidths of H atoms in $H_2$ films and their shifts from the positions of the ESR lines of the corresponding atoms in the gas phase.[11] By comparing of these two independent
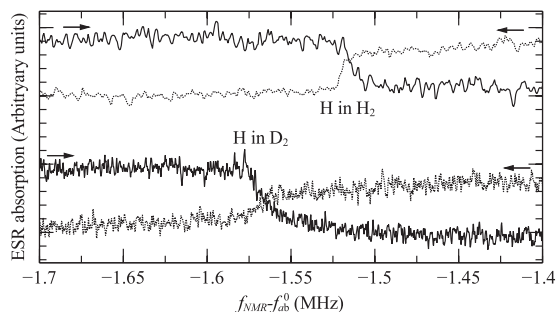
measurements, a conclusion regarding the distribution and possible clusterization of the stabilized atoms in $H_2$ ($D_2$) matrices can be established.

In conclusion, we have presented the design and performance of an experimental cell constructed for matrix isolation studies of H and D atomic radicals in solid molecular hydrogen and deuterium films at temperatures down to 70 mK. Smooth and homogeneous $H_2$ matrices of various thicknesses can be produced using a molecular beam deposition technique. High-density samples of atomic H and D radicals can be prepared for studies of macroscopic quantum phenomena and exchange tunneling reactions. Current design allows weighing the $H_2$ ($D_2$) films with 0.2 monolayer precision and simultaneously studying atomic free radicals stabilized in the solid $H_2$ and $D_2$ matrices by high frequency electron-spin and nuclear magnetic resonance. Calorimetric calibration of the ESR signal permits determination of the distribution of stabilized atoms in the $H_2$ ($D_2$) films.

FIG. 9. ENDOR spectra for H atoms in $H_2$ (upper lines) and $D_2$ matrices (lower lines). $f_{ab}^0$ is the free H atom $a$–$b$ transition frequency. The arrows denote the sweep direction. For details of ENDOR experiment see Ref. 11.

[1]M. E. Fajardo, *in Physics and Chemistry at Low Temperatures*, edited by L. Khriachtchev (Pan Stanford, 2011), pp. 167–202.
[2]U. Albrecht, H. Dilger, P. Leiderer, and K. Kono, Physica B **165–166**(2), 841 (1990).
[3]M. Sohaili, J. Klier, and P. Leiderer, J. Phys.: Condens. Matter **17**, S415 (2005).
[4]U. Albrecht, P. Evers, and P. Leiderer, Surf. Sci. **283**, 419 (1993).
[5]S. Ben-Ezra and W. I. Glaberson, Physica B **329-333**(1), 250 (2003).
[6]J. A. Phillips, D. Ross, P. Taborek, and J. E. Rutledge, Phys. Rev. B **58**, 3361 (1998).
[7]M. Moskovits and G. A. Ozin, Appl. Spectrosc. **26**, 481 (1972).
[8]A. Schrimpf, G. Sulzer, H.-J. Stöckmann, and H. Ackermann, Z. Phys. B **67**, 531 (1987).
[9]V. V. Khmelenko, D. M. Lee, and S. Vasiliev, in *Physics and Chemistry at Low Temperatures*, edited by L. Khriachtchev (Pan Stanford, 2011), pp. 107–166.
[10]J. Ahokas, J. Järvinen, V. V. Khmelenko, D. M. Lee, and S. Vasiliev, Phys. Rev. Lett. **97**, 095301 (2006).
[11]J. Ahokas, O. Vainio, S. Novotny, J. Järvinen, V. V. Khmelenko, D. M. Lee, and S. Vasiliev, Phys. Rev. B **81**, 104516 (2010).
[12]J. Ahokas, O. Vainio, J. Järvinen, V. V. Khmelenko, D. M. Lee, and S. Vasiliev, Phys. Rev. B **79**, 220505 (2009).
[13]S. Vasilyev, J. Järvinen, E. Tjukanoff, A. Kharitonov, and S. Jaakkola, Rev. Sci. Instrum. **75**, 94 (2004).
[14]D. Salt, *The Hy-Q Handbook of Quartz Crystal Devices* (Van Nostrand Reinhold (UK) Company Limited, 1986).
[15]LIT-Phonon, Moscow, Russia.
[16]M. Lea, P. Fozooni, and P. Retz, J. Low Temp. Phys. **54**, 303 (1984).
[17]J. F. Reichert and N. C. Jarosik, Phys. Rev. B **27**, 2710 (1983).
[18]R. van Roijen, J. Berkhout, B. Hebral, and J. T. M. Walraven, "A cryogenic dissociator for atomic hydrogen," (unpublished).
[19]J. Järvinen, J. Ahokas, and S. Vasiliev, J. Low Temp. Phys. **147**, 579 (2007).
[20]F. J. Adrian, J. Chem. Phys. **32**, 972 (1960).